LAWRENCE LIVERMORE NATIONAL LABORATORY

LLNL-CONF-643935

Characterization of a megapixel CMOS charge dump and read camera

J. R. Kimbrough, P. M. Bell, P. S. Datte, M. S. Thao, E. O. Vergel de Dios, A. S. Peters

September 17, 2013

SPIE
San Diego, CA, United States
August 25, 2013 through August 29, 2013

Characterization of a megapixel CMOS charge dump and read camera

Joseph R. Kimbrough*[a], P. M. Bell[a], P. S. Datte[a], M. S. Thao[a], E. O. Vergel de Dios[a], A. S. Peters[b]
[a]Lawrence Livermore National Laboratory, 7000 East Ave, Livermore, CA USA 94551-0808
[b]Spectral Instruments, 420 Bonita Ave, Tucson, AZ USA 85745

ABSTRACT

The National Ignition Facility requires a radiation-hardened, megapixel CMOS imaging sensor-based camera to be a direct physical and operational replacement for the CCD cameras currently used in x-ray streak cameras and gated imaging detectors. Camera electronics were selected to operate up to 10 krad(Si). The camera incorporates a fast dump of the sensor followed by exposure and image readout. This allows the dumping of charge due to the prompt radiation background and then readout of the longer persistence phosphor image from the x-ray diagnostics. Internal timing delays and optical performance were measured for a radiation-tolerant camera, based on the 2k by 2k CMV4000 sensor from CMOSIS Inc.

Keywords: CMOS imager, CCD camera, charge dump, radiation tolerant.

1. INTRODUCTION

The National Ignition Facility uses x-ray streak cameras and gated x-ray cameras to provide spatial and time resolved images of inertial confinement fusion implosions. Common to both diagnostics is the use of a gated microchannel plate and phosphor, coupled by a fiber optic to either a scientific grade megapixel CCD camera or film. The primary readout system used in these NIF diagnostics is a Spectral Instruments 1000 series[1] CCD camera. The camera was designed to fit into the NIF standard diagnostic airbox cross section and image the same area as the unsprocketed 35mm film pack. The 14 MeV neutrons produced by the capsule interact with material in the target chamber, including the diagnostic creating protons, alpha particles, and gamma radiation. This radiation creates charges in the pixels, excites the output phosphor, and creates Cherenkov radiation in the fiber optic bundle. Of those noise sources, the dominant source of background noise in the readout image is due to charge induced in the CCD pixel. The bright spots and background noise in the CCD will scale up with increasing neutron yields (see Figure 1). Radiation tests at the Omega laser at LLE with a Kodak 16800 CCD[2] gave an operational limit of 10^8 n/cm^2 due to the increasing background noise. Figure 1 shows the simulated degradation of the CCD image due to radiation induced noise[3].

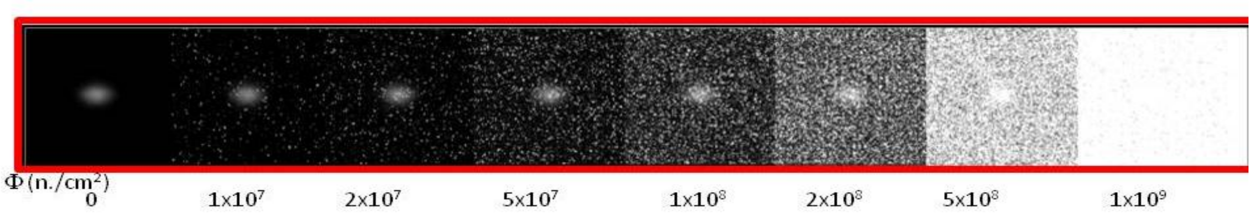

Figure 1. Actual CCD image of implosion with simulate noise due to radiation.

One way to reduce the radiation induced noise is to dump the charge in the pixels until the neutrons and gamma pulses have passed. Following the radiation pulse quickly acquire an image of the output phosphor before the phosphor image intensity decays[4]. The complete dump and read plot (see Figure 2) is for an imaging system using P20 phosphor and a read time based on the Spectral Instruments Model 1050 camera. This method requires the image sensor to have a global reset capability: the ability to quickly dump the unwanted charge at the pixel level.

*kimbrough1@llnl.gov

In addition to increasing signal-to-noise on the output, it is important to minimize radiation effects on sensor readout and control electronics to prevent data loss during readout and mitigate long-term damage effects. These requirements are met by replacing the CCD sensor and its control electronics with a CMOS APD (Active Pixel Device) imaging sensor and simpler control electronics.

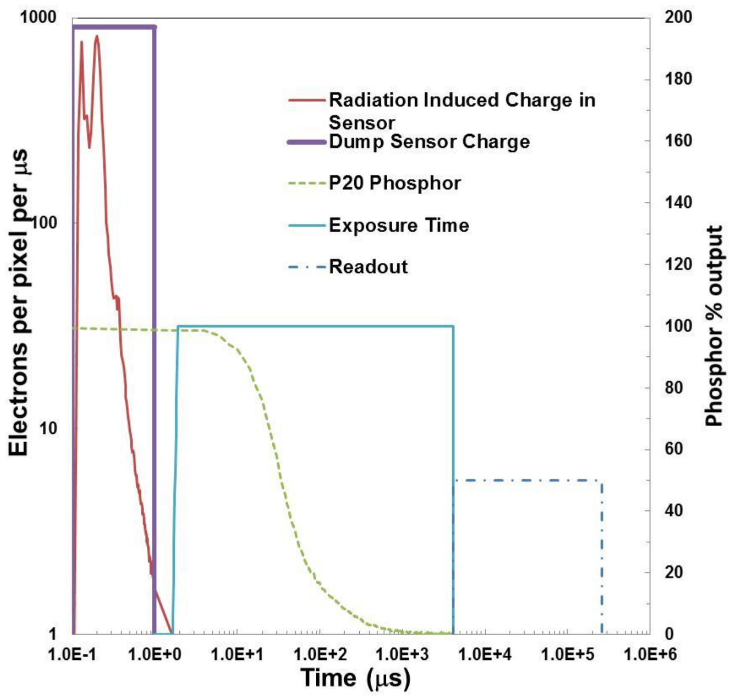

Figure 2. Plot showing timing of the charge dump due to radiation and subsequent imaging and readout of the phosphor signal.

2. DESCRIPTION

The Spectral Instruments 1050 series camera (see Figure 3) is a radiation-tolerant, fast dump camera, based on the CMOSIS CMV4000-2E5M0PN sensor. For radiation effects testing the sensor is bare and the camera has a Nikon lens mount. The camera uses the SI1000 camera interface and software for operation at NIF. The camera has both electrical and optical triggers, the ability to read out an image in ≈ 250 ms over fiber optic, and operate in a thermo-electrically cooled mode down to -40C. The cooled mode is available to minimize dark current noise due to temperature and radiation damage.

The user has the ability to select four analog gains (between 1.0X and 1.6X) and adjust the delay (“dump”) time between the camera trigger and acquisition of the desired image. The delay time is in increments of 50 ns with a range of 100 ns to 3.28 ms. Pixels are held in reset mode, removing the radiation induced electrons, until the specified integration delay is completed. Once the delay is complete the camera sets the pixels to exposure mode for the specified time and then reads out the image. In this camera the exposure mode range is 1 ms to 65.5 second in 1ms steps.

The camera electronics were chosen to provide an estimated 10 krad(Si) of radiation hardness. Parts were selected based on a review of radiation effect reports and databases. If there was no test data for a particular device then data from that family of devices was used. Control and readout of the sensor is through an Actel PE600L Field Programmable Gate Array (FPGA). This FPGA was used instead of the more costly hardened Actel RTPE600L which is part of the radiation-tolerant RT ProASIC family. Both parts incorporate flash cells to store the FPGA configuration. Unlike SRAM (Static Random Access Memory) based FPGAs, flash cells showed no single event upset due to heavy ion radiation. The 3D Plus radiation-tolerant memory stores the program which runs on the FGPA microcontroller. This program runs the camera, doing communication, temperature control, sensor initialization and setup.

The CMV4000-2E5M0PN sensor has 8-transistor (8T) architecture with a pinned photodiode fabricated in 0.18 micron CMOS process with a 5 micron EPI layer[5]. The one inch square imaging area is composed of 2048 by 2048 active pixels on a 5.5 micron pitch. The 8T design provides global shutter, global reset, and double-correlated sampling capabilities. The advantage of the global shutter is that the pixel does not respond to light during read out. The global reset is required to dump the charge from the pixels. The pinned photodiode and the EPI layer should also contribute to a reduction of the image background noise due to radiation[6].

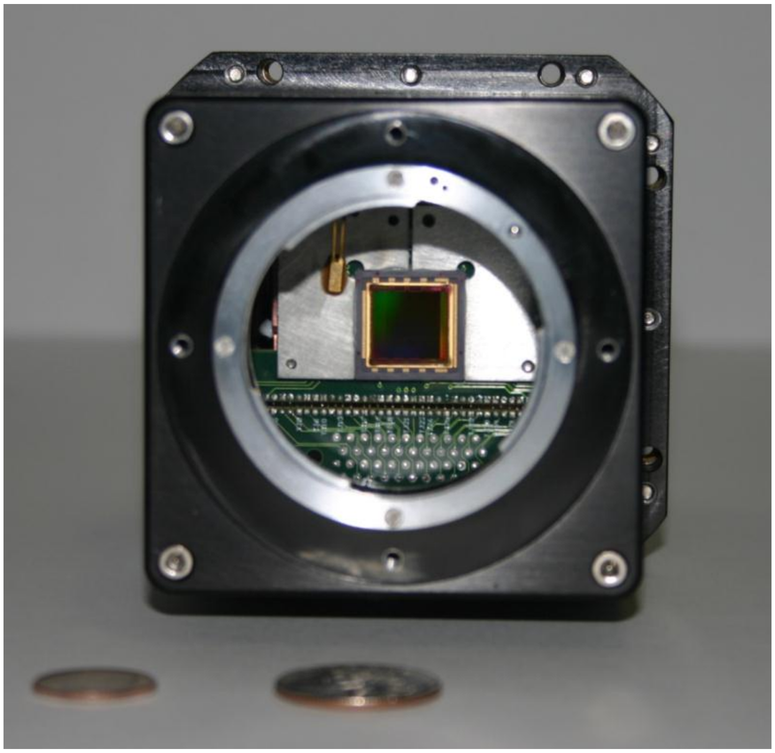

Figure 3. Front view of a Spectral Instruments Model 1050 camera showing the CMOSIS CMV4000 sensor.

3. METHODOLOGY

The radiation effects test plan consists of three steps. In the first step the classic photon transfer method was used to evaluate the camera performance. This step established the camera performance baseline in 2013. The second step is exposure of the operating camera to fluences up to $6x10^9$ n/cm^2 during deuterium/tritium fusion shots in the NIF target chamber in 2014. After each exposure the camera performance is characterized using dark and bright field images. At the end of exposure testing there is a repeat of the optical characterization to evaluate the effects of the radiation exposure on camera performance.

Use of the camera in a fast charge dump and read mode requires knowing the delay and jitter from the trigger signal into the camera to the start of exposure and the ability of the camera to fully dump the charge. A laser diode based test setup (see Figure 4) was used to determine both internal camera delay time and the sensor delay to actual start of the exposure. The actual start of the delay time and start of exposure will vary due to two clocks used in the camera. There is a 40 MHz (50 ns) clock to operate the FPGA state machine logic and a slower 8.33 MHz (120ns) clock to operate the sensor. The camera delay is set in 50 ns steps and the following exposure period in 1 msec steps. In order to reduce timing jitter, the timing measurements were done in two phases. The first phase characterized camera delays and jitter due to camera control logic from the trigger in signal to when the start of exposure signal reached the sensor. In the second phase, the timing of a 15ns full-width-half-max 60 pJ laser pulse is adjusted to move the laser pulse through the dump and exposure times (see Figure 5). Multiple images were taken at the rising edge, middle, and falling edges of the sensor clock. A 100 by 100 pixel array centered on the laser peak intensity was used to determine the average signal (see Figure 6). This latter test determines the actual time the sensor starts to see the laser after the falling edge of the start exposure signal.

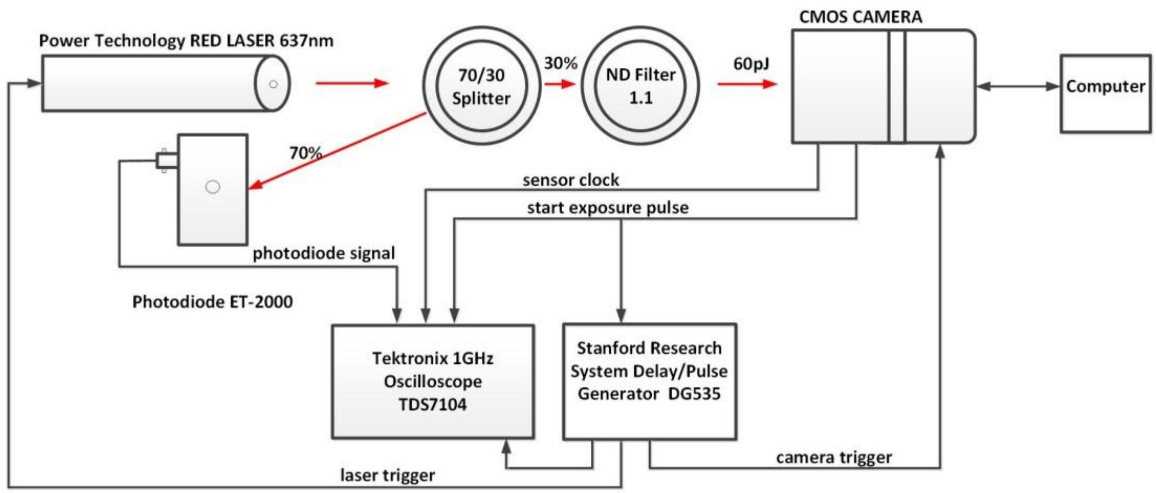

Figure 4. Test setup for sensor delays and actual start of exposure.

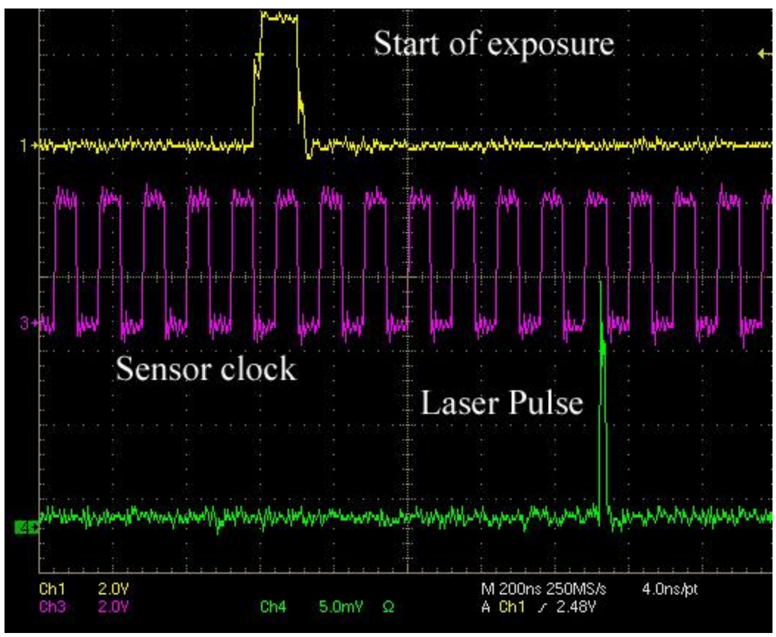

Figure 5. Showing start of exposure signal, sensor clock and laser pulse.

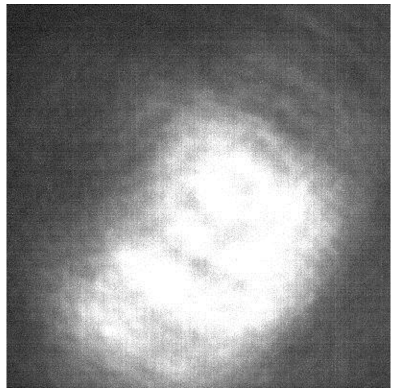

Figure 6. Averaged image of three of laser pulses.

4. RESULTS

In initial testing, the classic photon transfer method was used to evaluate the camera performance[7]. From this method we can determine the camera read noise, full well signal, dynamic range, and sensitivity shown in Table 1. Unity gain comparison shows the measured full well capacity is within 2.2% of the CMOSIS specification of 13.5k electrons. The timing tests and timing models showed that the delay from electrical trigger in to the start of exposure varied from 1040 ns to 1210 ns. This delay includes the seven clock cycles (840 ns) required after the start of exposure signal arrival at the chip before the sensor fully responds to light. The plot (see Figure 7) shows the average light intensity on the sensor for three laser pulses in terms of DN (Digital Number) versus the time the start of exposure signal arrived at the chip. The 170 ns variation has two causes. First is the variation in the arrival time of the camera trigger signal to the 50 ns clock edge. The second is the matching of the camera start exposure signal to the falling edge of the 120 ns sensor clock.

Table 1. Measured Camera Performance Specifications

Cam. Gain Setting	Cam. Gain Constant (e^-/DN)	Read Noise (e^-)	Full Well (e^-)	Dynamic Range
1.0X	4.6	23	13800	600
1.6X	2.6	21	9800	467

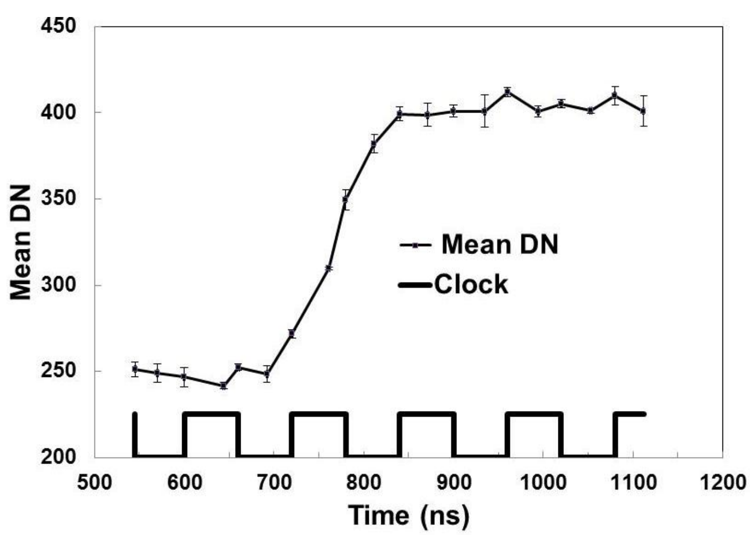

Figure 7. Plot shows the start of sensor response and the sensor clock.

At the end of the requested exposure time, the camera enables the sensor frame request signal to stop the exposure. The sensor remains sensitive to light for 133 μs after the sensor receives the frame request signal. The time the sensor remains sensitive to light after the arrival of the sensor frame request is consistent with the data sheet. In reading out the image there is a frame overhead time of 557 μs followed by 254 ms readout of the image.

5. CONCLUSION

These results show the series 1050 CMOS-based camera can be a replacement for the current 1000 series CCD-based camera. The dynamic range of 600 is more than sufficient to meet the dynamic range requirement of 300 due to the microchannel plates used in the NIF x-ray diagnotics[8]. The 170ns variation in time between trigger and actual start of exposure is acceptable for current applications. This variation can be reduced by changing the sensor clock from 8.33 MHz to 48 MHz. The operating software and mechanical interface allows for a virtually seamless transition from the 1000 series cameras. The radiation testing will validate the performance of this camera in the required NIF environment.

ACKNOWLEDGMENTS

I wish to acknowledge Spectral Instruments team for the design, build and testing of the model 1050 charge dump and read camera.

This work performed under the auspices of the U.S. Department of Energy by Lawrence Livermore National Laboratory under Contract DE-AC52-07NA27344, LLNL-CONF-642889

REFERENCES

[1] Kimbrough, J. R, Moody, J. D., Bell, P. M., Landen, O. L., “Characterization of the Series 1000 Camera System,” Rev. Sci. Instrum. 75, 4060-4062 (2004)

[2] Izumi, N., Hagmann, C., Stone, G., Hey, D., Glenn, S., Conder, A., Teruya, A., Sorce, C., Tommasini, R., Stoeffl, W., Springer, P., Landen, O. L., Herrmann, H. W., Kyrala, G. A., Bahukutumbi, R., Glebov, V., Y., Sangster, T. C., Eckart, M., Mackinnon, A. J., Koch, J. A., Bradley, D. K., and Bell, P., “Experimental study of neutron induced background noise on gated x-ray framing cameras,” Rev. Sci. Instrum. 81, 10E515-1-10E515-3 (2010)

[3] Hagmann, C., Izumi, N., Bell, P., Bradley, D., Conder, A., Eckart, M., Khater, H., Koch, J., “Modeling of neutron induced backgrounds in x-ray framing cameras,” Rev. Sci. Instrum. 81, 10E514-1-10E514-3 (2010)

[4] Izumi, N., et al., “Efficiency and decay time measurement of phosphors for x-ray framing cameras usable in harsh radiation background,” SPIE Vol. 8142, 81420I1-81420I6 (2011)

[5] Wang, X., Bogaerts, J., Vanhorebeek, G., Ruythoren, K., Ceulemans, B., Lepage, G., Willems, P., and Meynants, G., “A 2.2M CMOS Image Sensor for High Speed Machine Vision Applications,” SPIE Vol. 7536, 75360M1-75360M7 (2010)

[6] Wang, X., Bogaerts, J., Ogiers, W., Beeckman, G., and Meynant, G., “Design and characterization of radiation tolerant CMOS image sensor for space applications,” Proc. SPIE Vol. 8194, 81942N1-81942N6 (2011)

[7] Kimbrough, J. R., Moody, J. D., Bell, P., "Design and testing of a mega pixel charge dump and read camera," SPIE Vol. 8505, 85050D-1-8505D-7 (2012)
[8] Landen, O. L., Bell, P. M., Oertel, J. A., Satariano, J. J., and Bradley, D. K.," Gain uniformity, linearity, saturation, and depletion in gated microchannel-plate x-ray framing cameras," SPIE Vol. 2002, 1-13 (1993)